

Quantum Teleportation in High Dimensions

Yi-Han Luo,^{1,2} Han-Sen Zhong,^{1,2} Manuel Erhard,^{3,4} Xi-Lin Wang,^{1,2} Li-Chao Peng,^{1,2} Mario Krenn,^{3,4}
Xiao Jiang,^{1,2} Li Li,^{1,2} Nai-Le Liu,^{1,2} Chao-Yang Lu,^{1,2,*} Anton Zeilinger,^{3,4,†} and Jian-Wei Pan^{1,2,‡}

¹Hefei National Laboratory for Physical Sciences at Microscale and Department of Modern Physics,
University of Science and Technology of China, Hefei, 230026, China

²CAS Centre for Excellence in Quantum Information and Quantum Physics, Hefei, 230026, China

³Austrian Academy of Sciences, Institute for Quantum Optics and Quantum Information (IQOQI),
Boltzmannngasse 3, A-1090 Vienna, Austria

⁴Vienna Center for Quantum Science and Technology (VCQ), Faculty of Physics, University of Vienna, A-1090 Vienna, Austria



(Received 20 June 2019; published 15 August 2019)

Quantum teleportation allows a “disembodied” transmission of unknown quantum states between distant quantum systems. Yet, all teleportation experiments to date were limited to a two-dimensional subspace of quantized multiple levels of the quantum systems. Here, we propose a scheme for teleportation of arbitrarily high-dimensional photonic quantum states and demonstrate an example of teleporting a qutrit. Measurements over a complete set of 12 qutrit states in mutually unbiased bases yield a teleportation fidelity of 0.75(1), which is well above both the optimal single-copy qutrit state-estimation limit of 1/2 and maximal qubit-qutrit overlap of 2/3, thus confirming a genuine and nonclassical three-dimensional teleportation. Our work will enable advanced quantum technologies in high dimensions, since teleportation plays a central role in quantum repeaters and quantum networks.

DOI: 10.1103/PhysRevLett.123.070505

The laws of quantum mechanics forbid precise measurement or perfect cloning of unknown quantum states [1]. With the help of shared entanglement and classical communication channel, however, quantum teleportation in principle allows faithful transfer of the unknown quantum states from one particle to another at a distance [2], without physical transmission of the object itself. There have been numerous experiments on the teleportation of quantum states of single photons [3–8], atoms [9], trapped ions [10,11], defects in solid states [12], and superconducting circuits [13]. All these quantum systems naturally possess not only multiple degrees of freedom (d.o.f.), but, also, many d.o.f. can have high quantum numbers [14] beyond the simplified two-level qubit subspace. However, all experiments to date were limited to two-dimensional subspaces, the qubits [3–13]. After the teleportation of a two-particle composite state [6] and two d.o.f. [7], the teleportation of high-dimensional (HD) quantum states remained the final obstacle for teleporting a quantum particle intact.

The ability of coherent control of high-dimensional quantum states is important for developing advanced quantum technologies. Compared to the conventional two-level systems, HD states can offer extended possibilities such as both higher capacity and noise resilience in quantum communications [15,16], more efficient quantum simulation [17] and computation [18], as well as larger violation of Bell inequality [19]. Recent years have witnessed an increasing capability to generate and measure HD entangled states [19–24]. However, the previous work

is predominantly limited in the coherent control of a single-particle HD state. A joint projection of two independent particles with unknown states into maximally entangled HD states, which requires some form of controlled interactions and will play a crucial role in the HD teleportation, dense coding, and quantum computing, is more challenging and remains largely unexplored experimentally.

Here, we propose an efficient and extendable scheme for teleportation of arbitrarily HD photonic quantum states, and we report the first experimental teleportation of a qutrit, which is equivalent to a spin-1 system. We start by describing our protocol of HD quantum teleportation. For the sake of simplicity, here we explain it using the example of a three-level system, where the underlying physics can be generalized to arbitrary N -level systems [25]. Suppose Alice wishes to teleport to Bob the quantum state

$$|\varphi\rangle_a = \alpha_0|0\rangle_a + \alpha_1|1\rangle_a + \alpha_2|2\rangle_a \quad (1)$$

of a single photon, where $|0\rangle$, $|1\rangle$, and $|2\rangle$ are encoded by three different paths of the photon [cf., Fig. 1(a)]; their subscripts label the photon, and their coefficients are complex numbers that fulfill $|\alpha_0|^2 + |\alpha_1|^2 + |\alpha_2|^2 = 1$. The quantum resource required for teleporting this state is a HD entangled state previously shared between Alice and Bob; for example,

$$|\psi_{00}\rangle_{bc} = \frac{1}{\sqrt{3}}(|00\rangle_{bc} + |11\rangle_{bc} + |22\rangle_{bc}). \quad (2)$$

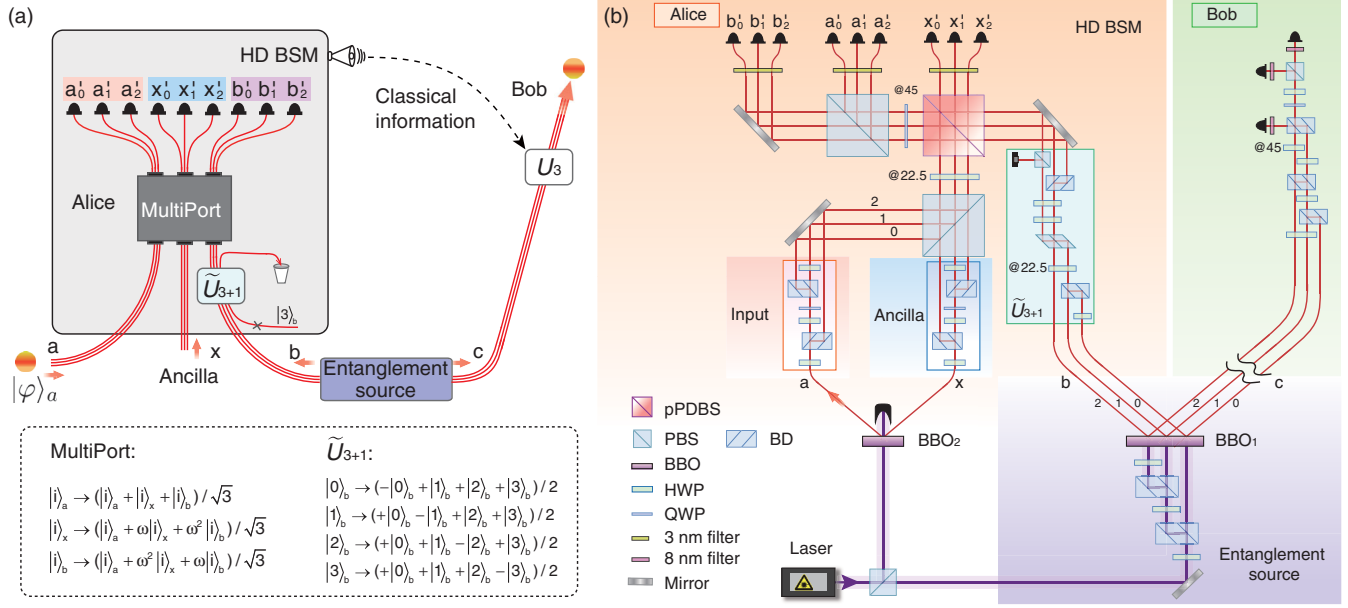


FIG. 1. (a) Principal scheme for teleportation of three-dimensional quantum states. Alice holds a quantum state $|\varphi_a\rangle$ encoded in three dimensions (depicted by three paths) that she wishes to teleport to Bob. To do so, they first share a three-dimensional, maximally entangled state. Then Alice performs a high-dimensional Bell-state measurement (HD BSM) on her photons. Conceptually, our approach upon realizing a HD BSM consists of two parts: a unitary transformation in an expanded state space (\tilde{U}_{3+1}) and a multiport beam splitter that enables collective quantum interference between Alice’s teleportee photon (a), her part of the entangled state (b), and an additional ancillary photon (x). Specific click patterns of different detectors indicate successful projections into one of the nine entangled Bell states. Alice can now transmit the classical information of her click pattern to Bob, who performs a unitary transformation (U_3) on his photon to recover the original state of Alice’s teleportee photon. (b) Experimental setup to teleport path-encoded qutrits. An ultraviolet pulsed laser is used to create a three-dimensionally entangled photon pair (path-encoded) in a nonlinear crystal (BBO₁) shared between Alice and Bob. The teleportee and ancillary photon are produced in a second nonlinear crystal (BBO₂). All 12 input qutrit states to be teleported and the ancilla photon are prepared using polarization-dependent beam displacers (BDs) controlled by half- and quarter-waver plates (HWP and QWP). The expanded unitary transformation \tilde{U}_{3+1} is implemented in a four-dimensional hybrid polarization-path state space. A polarizing beam splitter (PBS) traces out the additionally employed fourth dimension. All three photons (a , b , x) enter the three-dimensional multiport beam splitter, which consists of nested interferometers implemented in polarization and path d.o.f. A specifically designed partially polarizing beam splitter (PPDBS) ensures equally distributed input ports to all output ports. Simultaneous click-patterns of detectors $\{a'_0, a'_1, a'_2\}$, $\{b'_0, b'_1, b'_2\}$, or $\{x'_0, x'_1, x'_2\}$ indicate a successful BSM and herald a teleported photon at Bob’s side. No active feed-forward scheme was implemented here. Adjusting the HWP and QWP in Bob’s measurement apparatus allows for a complete analysis of the teleported qutrits.

This is one of the three-dimensional Bell states which, together with the other eight orthogonal ones [25], forms a complete orthonormal basis of the bipartite 3D Hilbert space.

Conceptually within the theoretical framework of Bennett *et al.* [2], the most crucial step for the HD teleportation is performing a joint measurement of photon a and b , a process called 3D Bell-state measurement (BSM). With equal probabilities of 1/9, the 3D BSM projects photon a and b into one of the nine 3D Bell states randomly. Alice can then broadcast the 3D BSM result classically, which allows Bob to accordingly apply a unitary single-particle 3D transform [30] to reconstruct the original quantum states [Eq. (1)] at his location [25]. In general, for an N -level bipartite system, there exists N^2 HD Bell states. An unambiguous HD BSM poses a new challenge both theoretically and experimentally.

Recall that in the teleportation of qubits, the four Bell states can be grouped into three symmetric and one

antisymmetric state under particle exchange, which facilitate the discrimination using linear optics [31]. In the 3D case already, however, the situation becomes fundamentally more complicated. There are three Bell states that are symmetric and the other six are neither symmetric nor antisymmetric. In theory, it was shown [32] that it is impossible to discriminate two-photon HD Bell states with linear optics only when the dimensions $N \geq 3$. To overcome such a linear optical limitation [32], here we utilize $N - 2$ additional single photons, so-called ancillary photons, and a multiport beam splitter with N -input– N -output all-to-all connected ports [33], which is a generalization of the quantum Fourier transform. A detailed derivation of the HD BSM procedure is shown in Ref. [25].

To get a deeper insight on how the high-dimensional Bell-state measurement works, we use the fact that in reverse a Bell state is generated. This simplifies the analysis

because in this case we can focus on one specific “click pattern” as an example, and send single photons backwards from these detectors. We choose to propagate three indistinguishable single photons from the output ports $\{a'_0, a'_1, a'_2\}$ backwards through the multiport, as shown in Fig. 1(a). Then we condition onto cases where in each input port one and only one photon exists. Because of the all-to-all connection in the multiport, the resulting state contains all length-two permutations of the 3D states [25]. Detection of the ancillary photon in the superposition state $(|0\rangle_x + |1\rangle_x + |2\rangle_x)/\sqrt{3}$ results in the obtained state (normalization omitted):

$$|0\rangle_a(|1\rangle_b + |2\rangle_b) + |1\rangle_a(|0\rangle_b + |2\rangle_b) + |2\rangle_a(|0\rangle_b + |1\rangle_b). \quad (3)$$

The unitary transformation of this state to a target 3D Bell state [Eq. (2)] requires an expanded Hilbert space of four dimensions. The extra fourth level $|3\rangle$ is added to assist the physical realization of the unitary transformation [see \tilde{U}_{3+1} in Fig. 1(a)], and erased afterwards, which leads to the target 3D Bell state [Eq. (2)] $|\psi_{00}\rangle_{bc}$ [25]. The analysis holds exactly the same if the three indistinguishable photons are “incident” from ports $\{b'_0, b'_1, b'_2\}$ or $\{x'_0, x'_1, x'_2\}$.

Thus, in the experiment, a simultaneous click of the three detectors in the ports $\{a'_0, a'_1, a'_2\}$, $\{b'_0, b'_1, b'_2\}$, or $\{x'_0, x'_1, x'_2\}$ indicates an unambiguous projection of the input photons a and b to the 3D Bell state $|\psi_{00}\rangle_{ab}$, which projects Bob’s photon c onto $|\varphi\rangle_c = \alpha_0|0\rangle_c + \alpha_1|1\rangle_c + \alpha_2|2\rangle_c$. This state is already identical to the original state of photon a without the need of any additional unitary corrections. The success probability of the HD BSM using this scheme is $1/81$. Combining with active feed-forward techniques increases the success probability to $1/9$ for linear optics [25].

Figure 1(b) shows the experimental setup for the 3D quantum teleportation. A femtosecond pulsed laser beam is split into two parts to simultaneously create two photon pairs. The first part of the pump beam is divided into three paths by two beam displacers which are then focused on the same β -borate-borate (BBO₁) crystal. We select the case where in total one photon pair is produced by type-II beamlike spontaneous parametric down-conversion [34], but without knowing at which one of the three paths, which generates the desired entangled state $|\psi_{00}\rangle_{bc}$ used as the quantum channel for the 3D teleportation. To ensure long-term phase stability between the three paths, we specifically design and fabricate interferometers with small (4 mm) separation between the three paths. Hence, air fluctuations and disturbances act collectively on all paths such that the qutrits are effectively protected in a decoherence-free space.

Before being sent to the HD BSM, photon b from the entangled qutrits first undergoes the unitary transformation

\tilde{U}_{3+1} , which is experimentally realized using a network of polarizing beam splitters and half-wave plates (HWPs). The details are shown in Supplemental Material [25]. Another pump beam from the same laser passes through BBO₂ and creates the second photon pair. One of them is used for the preparation of an arbitrary superposition of the three paths as the input state a to be teleported. The other one is used as the ancillary qutrit x in the HD BSM.

The experimental realization of the HD BSM puts stringent technological requirements on phase stability, efficiency, and precision. To meet these demands, the HD BSM is operated in hybrid polarization-path encoding and employs a fully connected three-input and three-output ultralow-loss multiport interferometer. As shown in Fig. 1(b), in the input, single photons a and b are initialized in horizontal polarization, while photon x is in vertical polarization. Photon a is first combined with photon x using a polarizing beam splitter (PBS). The combined beams pass through a HWP set at 22.5° , and are superposed with photon b on a partially polarization-dependent beam splitter (PPDBS), which totally reflects vertically polarized photons and partially, with a ratio of $1/3$, reflects horizontally polarized photons. One of the output ports of the PPDBS is detected by three detectors directly, while the other port is further sent through a quarter-wave plate set at 45° and then split by a polarizing beam splitter and detected by six detectors. It is straightforward to check that all the three photons from the inputs a , b , and x are evenly distributed to each of the outputs with a ratio of $1/3$, realizing the most important function of the multiport.

The all-to-all multiport in Fig. 1(b) involves three-photon nine-path Hong-Ou-Mandel interferences at the polarizing beam splitter and the PPDBS. All nine paths are synchronized to arrive within ~ 10 fs of each other, a delay much smaller than the coherence time of the narrow band (3 nm) filtered single photons (~ 450 fs). The use of compact and precisely aligned beam displacers ensures a good spatial overlap in all multipath interferences simultaneously. Verifications of all two-photon Hong-Ou-Mandel interference combinations at the PPDBS with an average visibility of $0.82(1)$ are presented in Supplemental Material [25]. These visibilities in combination with the entanglement source [with a measured fidelity of $0.94(1)$] quantify the quality of the three-dimensional teleportation experiment [25].

It is necessary to prove that the teleportation experiment works universally for all possible superposition states in the general form of $|\varphi\rangle_a$ [Eq. (1)] and has a performance exceeding that using only classical methods. Classically, the optimal single-copy state-estimation fidelity of a three-level quantum system [35] is 0.5 when averaging over the whole Hilbert space. Sampling only over partial state space in biased bases, however, would allow the classical strategy to make use of the biased information to obtain an average state estimation fidelity higher than 0.5 . It is therefore

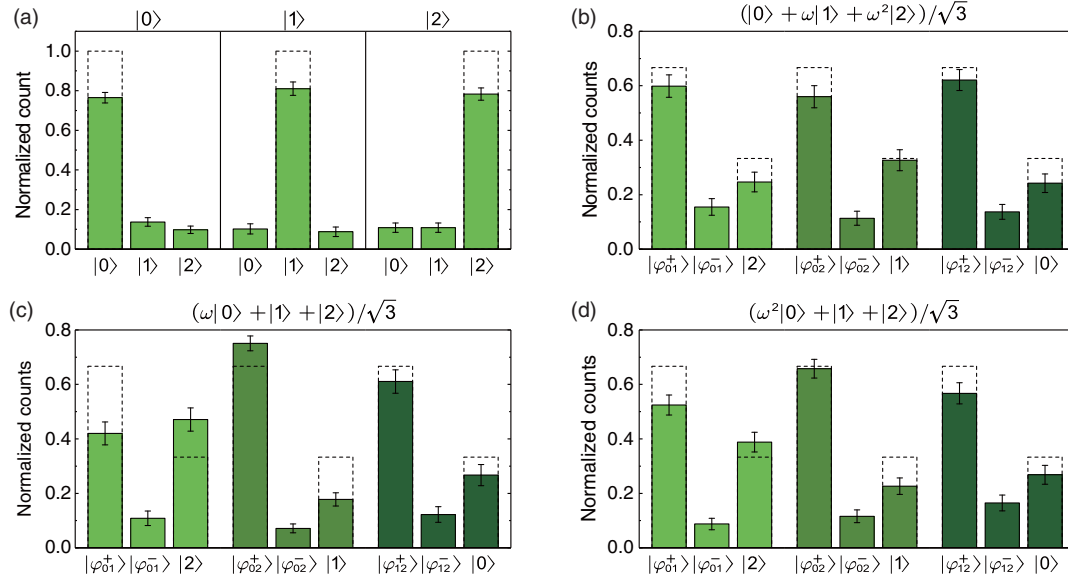


FIG. 2. Experimental results of qutrit teleportation. Measurement results for 6 out of all 12 basis states from different mutually unbiased bases groups $B_{\{1,2,3\}}^{(1-4)}$ for calculating the fidelities are displayed. Dashed empty bars indicate ideal measurement result for comparison. (a) All three computational basis states from the group $B_{\{1,2,3\}}^{(1)}$ and their relative four-photon occurrences are shown. (b)–(d) Measurement result of coherent superposition states from mutually unbiased bases groups $B_{\{1,2,3\}}^{(2)}$, $B_{\{1,2,3\}}^{(3)}$, and $B_{\{1,2,3\}}^{(4)}$, respectively. The different measurement outcomes $|\varphi_{ij}^{\pm}\rangle$ represent all possible two-dimensional combinations with phases according to the prepared qutrit state. Error bars are calculated using Monte Carlo simulation with an underlying Poissonian count rate distribution.

important to carefully choose a minimal set of input states such that the random sampling of which leads to the same classical limit as sampling over the whole state space. Such a minimal set of states lies in mutually unbiased bases [36]. For a three-dimensional system, we need to measure 12 states from four mutually unbiased bases:

$$\begin{aligned}
 B_{\{1,2,3\}}^{(1)} &: (1, 0, 0), (0, 1, 0), (0, 0, 1), \\
 B_{\{1,2,3\}}^{(2)} &: (1, 1, 1), (1, \omega, \omega^2), (1, \omega^2, \omega), \\
 B_{\{1,2,3\}}^{(3)} &: (\omega, 1, 1), (1, \omega, 1), (1, 1, \omega), \\
 B_{\{1,2,3\}}^{(4)} &: (\omega^2, 1, 1), (1, \omega^2, 1), (1, 1, \omega^2). \quad (4)
 \end{aligned}$$

Here the vectors $(\alpha_0, \alpha_1, \alpha_2)$ denote the state $\alpha_0|0\rangle_c + \alpha_1|1\rangle_c + \alpha_2|2\rangle_c$, and $\omega = \exp(i2\pi/3)$, where the normalizing constant is omitted. We measure fidelities of the final teleported states, defined as the overlap of the experimentally measured density matrix ρ_c with the ideal input state $|\psi\rangle_a$, which can be written as $\text{Tr}(|\psi\rangle\langle\psi|\rho)$. Conditioned on the detection of a specific click pattern within the HD BSM [see Fig. 1(a)], we register the counts of Bob's photon and analyze its properties. The verifications of the teleportation results are based on fourfold coincidence detections which in our experiment occur with a rate of 0.11 Hz. In each setting, the typical data accumulation time is 20–40 min, which allows us to sufficiently suppress Poisson noise.

Figure 2(a) shows the teleportation results of group $B_{\{1,2,3\}}^{(1)}$, which can be straightforwardly measured in the computational basis. The extracted fidelities are 0.76(3), 0.81(3), and 0.78(3) for the teleported state $|0\rangle$, $|1\rangle$, and $|2\rangle$, respectively. However, the measurements for the other three groups, which involves equal superpositions of all the three levels, are more complicated. To experimentally access the fidelity of these states in the general form,

$$|\phi\rangle = \frac{1}{\sqrt{3}}[|0\rangle + \exp(i\phi_1)|1\rangle + \exp(i\phi_2)|2\rangle], \quad (5)$$

we decompose the density matrix into three parts, $\rho = (\sigma_{012} + \sigma_{021} + \sigma_{120})/3$, where

$$\begin{aligned}
 \sigma_{ijk} &= |\varphi_{ij}^+\rangle\langle\varphi_{ij}^+| - |\varphi_{ij}^-\rangle\langle\varphi_{ij}^-| + |k\rangle\langle k|, \\
 |\varphi_{ij}^{\pm}\rangle &= [|i\rangle \pm \exp(i\phi_j - i\phi_i)|j\rangle] / \sqrt{2}.
 \end{aligned}$$

The decomposition unitarily transforms the qutrits into two-dimensional superposition states and one computational state. Our measurement apparatus allows a simultaneous three-outcome readout, directly accessing one of the σ_{ijk} [25]. We show in Figs. 2(b)–2(d) the measurement results for three representative states from the group of $B_{\{1,2,3\}}^{(2)}$, $B_{\{1,2,3\}}^{(3)}$, and $B_{\{1,2,3\}}^{(4)}$, respectively. The other six states are presented in Supplemental Material [25]. We note that all reported measurements are without background or

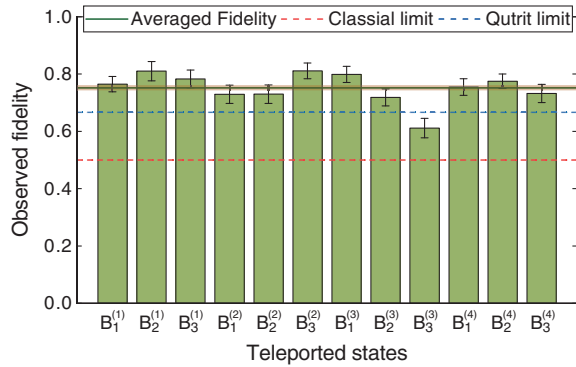


FIG. 3. Data summary for demonstrating a universal, non-classical, and genuine qutrit teleportation experiment. Here the fidelities of all 12 basis states are listed to demonstrate universality. Our average achieved fidelity of 0.75(1) significantly overcomes both the nonclassical bound of $1/2$ and the genuine qutrit bound of $2/3$. The shaded area is 1 standard deviation of the average fidelity. Error bars for fidelities are calculated with a Monte Carlo simulation and an underlying Poissonian distribution of photon counts. Gaussian error propagation yields the error for the average fidelity.

accidental count subtraction. The fidelity imperfection is mainly from double pair emissions, spatial mode mismatch in the multiphoton multipath interferences, and interferometric noise in the state preparation and measurements [25].

The fidelities of all the 12 states are displayed in Fig. 3, which are the minimal set allowing us to faithfully derive the teleportation fidelity for the three-level quantum system. In the current experiment, the averaged fidelity is calculated to be 0.75(1), well above the classical limit of 0.5 which can be obtained with the best classical strategy.

Proving the universality and nonclassicality is already sufficient for teleporting qubits. However, for the N -dimensional teleportation, it is important to further verify that all N dimensions still can form a coherent superposition and thus survived the teleportation intact. Hence, a genuine N -dimensional teleportation should be distinguished from lower-dimensional cases by excluding the hypotheses that the teleported state could be represented with less dimensions. For our specific 3D teleportation, we can calculate that the maximal overlap between any two-level superposition and the genuine three-level states is $2/3$ [25]. The teleportation fidelity measured in our work exceeds this threshold by 9 standard deviations, thus conclusively establishing a genuine three-dimensional quantum teleportation.

To summarize, we have for the first time demonstrated the possibility to completely teleport the multiple quantized levels of a quantum system. Our generalized scheme [25] can readily be applied to other d.o.f., such as the photon's orbital angular momentum [37]. Future scaling up to higher dimensions would be suitable to be implemented in integrated photonics platforms [22,24]. It would also be interesting to investigate in the future the teleportation of

multiple atomic levels in trapped ions [10,11] and cold atoms [9]. An intriguing idea appears upon combining our approach with the teleportation of a two-particle composite state [6] and 2 d.o.f. [7], which makes it possible to realize the dream of teleporting a complex quantum system completely.

The ability to perform the HD BSM developed in this work provides a new possibility for the fundamental test of Bell's inequalities and advanced quantum information technologies. As an example, the to-be-teleported HD quantum state can itself be fully undefined, such as being part of a two-particle HD entanglement. This leads to entanglement swapping [38], where heralded by a HD BSM click, two remote HD particles can be entangled with no direct interaction. Such a scheme can distribute entanglement over long distances and can enable an event-ready Bell test. Remarkably, the created HD entanglement can tolerate a higher detection inefficiency than the qubit case [19,39], and would provide significant advantages in a long-distance Bell test closing both locality and detection loopholes [40–42] and device-independent quantum key distribution [43].

This work was supported by the National Natural Science Foundation of China, the Chinese Academy of Sciences, the National Fundamental Research Program, and the Anhui Initiative in Quantum Information Technologies. M. E., M. K. and A. Z. are supported by the Austrian Academy of Sciences, the European Research Council (SIQS Grant No. 600645 EU-FP7-ICT), and the Austrian Science Fund (FWF) with SFB F40 (FoQuS) and FWF project W 1210-N25 (CoQuS), the Austrian Federal Ministry of Education, Science and Research (BMBWF) and the University of Vienna via the project QUESS. M. E. would like to thank C. Y. L. and J. W. P. for their hospitality during multiple stays in China. Y.-H. L., H.-S. Z., M. E., and X.-L. W. contributed equally to this work.

Note added.—Recently, we became aware of an independent experiment [44].

*cylu@ustc.edu.cn

†anton.zeilinger@univie.ac.at

‡pan@ustc.edu.cn

- [1] W. K. Wootters and W. H. Zurek, *Nature (London)* **299**, 802 (1982).
- [2] C. H. Bennett, G. Brassard, C. Crépeau, R. Jozsa, A. Peres, and W. K. Wootters, *Phys. Rev. Lett.* **70**, 1895 (1993).
- [3] D. Bouwmeester, J.-W. Pan, K. Mattle, M. Eibl, H. Weinfurter, and A. Zeilinger, *Nature (London)* **390**, 575 (1997).
- [4] A. Furusawa, J. L. Sørensen, S. L. Braunstein, C. A. Fuchs, H. J. Kimble, and E. S. Polzik, *Science* **282**, 706 (1998).
- [5] I. Marcikic, H. de Riedmatten, W. Tittel, H. Zbinden, and N. Gisin, *Nature (London)* **421**, 509 (2003).

- [6] Q. Zhang, A. Goebel, C. Wagenknecht, Y.-A. Chen, B. Zhao, T. Yang, A. Mair, J. Schmiedmayer, and J.-W. Pan, *Nat. Phys.* **2**, 678 (2006).
- [7] X.-L. Wang, X.-D. Cai, Z.-E. Su, M.-C. Chen, D. Wu, L. Li, N.-L. Liu, C.-Y. Lu, and J.-W. Pan, *Nature (London)* **518**, 516 (2015).
- [8] J.-G. Ren *et al.*, *Nature (London)* **549**, 70 (2017).
- [9] X.-H. Bao, X.-F. Xu, C.-M. Li, Z.-S. Yuan, C.-Y. Lu, and J.-W. Pan, *Proc. Natl. Acad. Sci. U.S.A.* **109**, 20347 (2012).
- [10] M. Riebe, H. Häffner, C. F. Roos, W. Hänsel, J. Benhelm, G. P. T. Lancaster, T. W. Körber, C. Becher, F. Schmidt-Kaler, D. F. V. James, and R. Blatt, *Nature (London)* **429**, 734 (2004).
- [11] M. D. Barrett, J. Chiaverini, T. Schaetz, J. Britton, W. M. Itano, J. D. Jost, E. Knill, C. Langer, D. Leibfried, R. Ozeri, and D. J. Wineland, *Nature (London)* **429**, 737 (2004).
- [12] W. Pfaff, B. J. Hensen, H. Bernien, S. B. van Dam, M. S. Blok, T. H. Taminiau, M. J. Tiggelman, R. N. Schouten, M. Markham, D. J. Twitchen, and R. Hanson, *Science* **345**, 532 (2014).
- [13] L. Steffen, Y. Salathe, M. Oppliger, P. Kurpiers, M. Baur, C. Lang, C. Eichler, G. Puebla-Hellmann, A. Fedorov, and A. Wallraff, *Nature (London)* **500**, 319 (2013).
- [14] R. Fickler, R. Lapkiewicz, W. N. Plick, M. Krenn, C. Schaeff, S. Ramelow, and A. Zeilinger, *Science* **338**, 640 (2012).
- [15] N. J. Cerf, M. Bourennane, A. Karlsson, and N. Gisin, *Phys. Rev. Lett.* **88**, 127902 (2002).
- [16] I. Ali-Khan, C. J. Broadbent, and J. C. Howell, *Phys. Rev. Lett.* **98**, 060503 (2007).
- [17] M. Neeley, M. Ansmann, R. C. Bialczak, M. Hofheinz, E. Lucero, A. D. O'Connell, D. Sank, H. Wang, J. Wenner, A. N. Cleland, M. R. Geller, and J. M. Martinis, *Science* **325**, 722 (2009).
- [18] B. P. Lanyon, M. Barbieri, M. P. Almeida, T. Jennewein, T. C. Ralph, K. J. Resch, G. J. Pryde, J. L. O'Brien, A. Gilchrist, and A. G. White, *Nat. Phys.* **5**, 134 (2009).
- [19] D. Collins, N. Gisin, N. Linden, S. Massar, and S. Popescu, *Phys. Rev. Lett.* **88**, 040404 (2002).
- [20] M. Krenn, M. Huber, R. Fickler, R. Lapkiewicz, S. Ramelow, and A. Zeilinger, *Proc. Natl. Acad. Sci. U.S.A.* **111**, 6243 (2014).
- [21] Z. Xie, T. Zhong, S. Shrestha, X. Xu, J. Liang, Y.-X. Gong, J. C. Bienfang, A. Restelli, J. H. Shapiro, F. N. Wong, and C. W. Wong, *Nat. Photonics* **9**, 536 (2015).
- [22] M. Kues, C. Reimer, P. Roztocky, L. R. Cortés, S. Sciara, B. Wetzell, Y. Zhang, A. Cino, S. T. Chu, B. E. Little, D. J. Moss, L. Caspani, J. Azaña, and R. Morandotti, *Nature (London)* **546**, 622 (2017).
- [23] M. Erhard, M. Malik, M. Krenn, and A. Zeilinger, *Nat. Photonics* **12**, 759 (2018).
- [24] J. Wang, S. Paesani, Y. Ding, R. Santagati, P. Skrzypczyk, A. Salavrakos, J. Tura, R. Augusiak, L. Mančinska, D. Bacco, D. Bonneau, J. W. Silverstone, Q. Gong, A. Acín, K. Rottwitt, L. K. Oxenløwe, J. L. O'Brien, A. Laing, and M. G. Thompson, *Science* **360**, 285 (2018).
- [25] See Supplemental Material at <http://link.aps.org/supplemental/10.1103/PhysRevLett.123.070505> for details, which includes Refs. [26–29].
- [26] J. Calsamiglia, *Phys. Rev. A* **65**, 030301 (2002).
- [27] R. Fickler, R. Lapkiewicz, M. Huber, M. P. Lavery, M. J. Padgett, and A. Zeilinger, *Nat. Commun.* **5**, 4502 (2014).
- [28] A. Hayashi, T. Hashimoto, and M. Horibe, *Phys. Rev. A* **72**, 032325 (2005).
- [29] H.-S. Zhong, Y. Li, W. Li, L.-C. Peng, Z.-E. Su, Y. Hu, Y.-M. He, X. Ding, W. Zhang, H. Li *et al.*, *Phys. Rev. Lett.* **121**, 250505 (2018).
- [30] M. Reck, A. Zeilinger, H. J. Bernstein, and P. Bertani, *Phys. Rev. Lett.* **73**, 58 (1994).
- [31] H. Weinfurter, *Europhys. Lett.* **25**, 559 (1994).
- [32] J. Calsamiglia, *Phys. Rev. A* **65**, 030301(R) (2002).
- [33] M. Żukowski, A. Zeilinger, and M. A. Horne, *Phys. Rev. A* **55**, 2564 (1997).
- [34] X.-L. Wang, L.-K. Chen, W. Li, H. L. Huang, C. Liu, C. Chen, Y. H. Luo, Z. E. Su, D. Wu, Z. D. Li, H. Lu, Y. Hu, X. Jiang, C. Z. Peng, L. Li, N. L. Liu, Y.-A. Chen, C.-Y. Lu, and J.-W. Pan, *Phys. Rev. Lett.* **117**, 210502 (2016).
- [35] D. Bruß and C. Macchiavello, *Phys. Lett. A* **253**, 249 (1999).
- [36] I. D. Ivanovic, *J. Phys. A* **14**, 3241 (1981).
- [37] A. M. Yao and M. J. Padgett, *Adv. Opt. Photonics* **3**, 161 (2011).
- [38] M. Żukowski, A. Zeilinger, M. A. Horne, and A. K. Ekert, *Phys. Rev. Lett.* **71**, 4287 (1993).
- [39] T. Vértesi, S. Pironio, and N. Brunner, *Phys. Rev. Lett.* **104**, 060401 (2010).
- [40] B. Hensen, H. Bernien, A. E. Dréau, A. Reiserer, N. Kalb, M. S. Blok, J. Ruitenberg, R. F. Vermeulen, R. N. Schouten, C. Abellán *et al.*, *Nature (London)* **526**, 682 (2015).
- [41] M. Giustina, M. A. M. Versteegh, S. Wengerowsky, J. Handsteiner, A. Hochrainer, K. Phelan, F. Steinlechner, J. Kofler, J.-Å. Larsson, C. Abellán *et al.*, *Phys. Rev. Lett.* **115**, 250401 (2015).
- [42] L. K. Shalm, E. Meyer-Scott, B. G. Christensen, P. Bierhorst, M. A. Wayne, M. J. Stevens, T. Gerrits, S. Glancy, D. R. Hamel, M. S. Allman *et al.*, *Phys. Rev. Lett.* **115**, 250402 (2015).
- [43] A. Acín, N. Gisin, and L. Masanes, *Phys. Rev. Lett.* **97**, 120405 (2006).
- [44] X.-M. Hu, C. Zhang, B.-H. Liu, Y.-F. Huang, C.-F. Li, and G.-C. Guo, [arXiv:1904.12249](https://arxiv.org/abs/1904.12249).